East European chironomid-based calibration model for past summer temperature reconstructions

Luoto, Tomi P.

2019

Luoto , T P , Kotrys , B & Plociennik , M 2019 , ' East European chironomid-based calibration model for past summer temperature reconstructions ' , Climate Research , vol. 77 , no. 1 , pp. 63-76 . https://doi.org/10.3354/cr01543

http://hdl.handle.net/10138/312767
https://doi.org/10.3354/cr01543

acceptedVersion

East European chironomid-based calibration model for past summer temperature reconstructions

Tomi P. Luoto[1,*], Bartosz Kotrys[2] and Mateusz Płóciennik[3]

[1]Faculty of Biological and Environmental Sciences, Ecosystems and Environment Research Programme, University of Helsinki, 15140 Lahti, Finland

[2]Polish Geological Institute - National Research Institute, Pomeranian Branch in Szczecin, 71-130 Szczecin, Poland

[3]Department of Invertebrate Zoology and Hydrobiology, Faculty of Biology and Environmental Protection, University of Lodz, 90-237 Lodz, Poland

[*]Corresponding author (e-mail: tomi.luoto@helsinki.fi)

Running page head: East European chironomid-temperature model

ABSTRACT: Understanding local patterns and large scale processes in past climate necessitates detailed network of temperature reconstructions. In this study, a merged temperature inference model using fossil chironomid (Diptera: Chironomidae) datasets from Finland and Poland was constructed to fill the lack of an applicable training set for East European sites. The developed weighted averaging-partial least squares (WA-PLS) inference model showed favorable performance statistics suggesting that the model can be useful for downcore reconstructions. The combined calibration model includes 212 sites, 142 taxa and a temperature gradient of 11.3-20.1 °C. The 2-component WA-PLS model has a cross-validated coefficient of determination of 0.88 and a root mean squared prediction error of 0.88 °C. We tested the new East European temperature transfer function in chironomid stratigraphies from a Finnish high-resolution short-core sediment record and a Polish paleolake (Żabieniec) covering the past ~20,000 yr. In the Finnish site, the chironomid-inferred temperatures correlated closely with the observed instrumental temperatures showing improved accuracy compared to estimates by the original Finnish calibration model. In addition, the long-core reconstruction from the Polish site showed logical results in its general trends compared to existing knowledge on the past regional climate trends, however, with distinct differences when compared with hemispheric climate oscillations. Hence, based on these findings, the new temperature model will enable more detailed examination of long-term temperature variability in Eastern Europe, and consequently reliable identification of local and regional climate variability of the past.

KEYWORDS: Chironomidae, Climate reconstruction, Finland, Holocene, Late Glacial, Paleoclimate, Poland, Training set, Transfer function

1. INTRODUCTION

Advances in paleoclimatology have enabled building of comprehensive outline of climate changes of the recent past, the Holocene epoch and the last Glacial cycle (McCarroll 2015, Wanner et al. 2015, Linderholm et al. 2018). However, the local differences and small-scale variation are still poorly established in several geographic areas. In addition to high-fidelity sediment archives, the paleoclimatological toolpack needs to be refined to tackle reliably the climate variability of the past. Non-biting midges (Insecta: Diptera: Chironomidae) have been recognized as one of the most powerful proxies to reconstruct past summer air temperature dynamics (Brooks 2006). Utilizing the fossil community compositions of the temperature-sensitive chironomid taxa and applying the calibration set approach via a transfer function, quantitative climate inferences have become available from sites where other paleoclimate proxies have failed or are not possible to use (Ilyashuk et al. 2011, Luoto et al. 2018). In addition to confounding environmental variables, such as nutrients (Quinlan & Brodersen 2006, Eggermont & Heiri 2012, Medeiros et al. 2015), a potential downside of chironomids as a paleotemperature proxy lays in the suitability of the calibration set to the downcore site (Engels et al. 2014). In an ideal situation, the downcore site should be within the geographical area of the training set, the study site characteristics (such as lake size and depth) should be similar and the calibration sites should constitute a temperature gradient that covers the expected range of past temperature changes. When applying inference models to cores outside the training set's geographical or environmental range, problems related to taxa occurrences (poor modern analogues) and unrealistic taxon-specific temperature optima arises. Moreover, continental scale calibration sets (Heiri et al. 2011) may not be able to detect small-magnitude variation in temperatures, although they can be very useful in reconstructing the large-scale climate patterns.

Previously, it has been challenging to produce reliable chironomid-based temperature inferences at the ends of the temperature gradient in Eastern Europe. In downcore sites located in southern Finland, temperatures of the warm climate events, such as the recent warming, Medieval Climate Anomaly and Holocene Thermal Maximum, may have been underestimated due to lack of equally warm calibration sites (Rantala et al. 2016, Shala et al. 2017). Similarly, the lack of warm calibration sites in the available chironomid-based temperature inference models have thus far caused problems in downcore studies of Polish sites due to deficiency of warm analogues (Pawłowski et al. 2015, 2016a). Here, we combine the Finnish calibration sets (Luoto 2009, Luoto et al. 2016) with a dataset collected from Poland (previously unpublished) to create a more applicable temperature inference model for East European sites than has previously been available. In addition to standard numerical testing of the model performance, we validate the model using a chironomid stratigraphy from an annually laminated lake sediment record from Finland and compare the reconstruction against instrumentally measured temperatures. In addition, we apply the East European calibration model on a chironomid record from a Polish paleolake covering the past ~20,000 yr and compare the output against previous reconstructions. We aim to produce a new quantitative tool for more reliable reconstructions of past climate patterns in the East European sector to better describe local climate variability.

2. MATERIAL AND METHODS

2. 1. Study sites and sediments

The training set study sites comprise of 212 lakes located in Finland and Poland (Fig. 1). The 114 Finnish sites, collected with a Limnos gravity corer between 2005 and 2014, originate from two previously published datasets located at a treeline transect in northeastern Lapland (32 lakes,

68°47' – 69°55'N) (Luoto et al. 2016) and along the latitudinal gradient of Finland (82 lakes, 60°13' – 69°53'N) (Luoto 2009). The mean July air temperature in the Finnish sites varies between 11.3 and 17.1 °C (mean 14.4 °C, median 14.1 °C) within an altitudinal gradient of 4-405 m a.s.l. All the sites are small and shallow (0.5-7.0 m) with pH between 4.6 and 8.4. The 98 Polish lakes, sampled in summer 2014 using a Kajak corer, are located between 49°19'–54°68'N and constitute an altitudinal gradient of 4-1624 m a.s.l. The mean July air temperature in the Polish sites varies between 11.6 and 20.1 °C (mean 18.6 °C, median 18.9 °C), whereas the depth range is 0.3-15.0 m. The lake water pH fluctuate between 5.1 and 9.8. The Polish dataset is previously unpublished. Comparison between the combined training sets is given in Table 1.

The short-core test site Lake Nurmijärvi (61°35'N, 25°55'E; 87.7 m a.s.l.) is located in south-central Finland (Fig. 1). The lake with annually laminated sediments is currently circumneutral (pH = 7.0) and mesotrophic. The mean July air temperature at the study site is 16.9 °C (climate normals 1981–2010, Finnish Meteorological Institute). The sediment sequence was cored in winter 2016 using a HTH-corer and subsampled at 1-cm intervals. The average sample interval in the verified varve chronology (Ojala et al. 2016, 2018) is 4 years and the available meteorological data begins from the 1830s. The full chironomid stratigraphy of Nurmijärvi is published (Luoto & Ojala 2016).

The long-core sediment site Żabieniec (51°51'N; 19°46'E; 180 m a.s.l.) is currently a bog located in central Poland (Fig. 1). The present-day mean July air temperature at the study site is 18 °C. Detailed descriptions of the study site and the paleolake sediments together with the full chironomid stratigraphy and chronology are given elsewhere (Płóciennik et al. 2011). In brief, the paleolake sediments were sampled using a piston corer and the subsampling was performed at varying intervals. The stratigraphy represents roughly the past 20,000 yr. The chronology of the core is based on 13 radiocarbon dates and the age-depth model is originally presented in Lamentowicz et al. (2009).

2.2. Chironomid analysis

Fossil chironomid analysis was performed using standard methods in all the datasets and cores applying provided guidelines (Brooks et al. 2007). In short, a 100 µm mesh was used for sieving at least 50 chironomid head capsules per sample. Similar to unidentified remains, other midges than chironomids were ignored. Taxonomic harmonization of the training sets and the two sediment downcores was achieved through close collaboration between the chironomid analysts. The morphologically similar taxa *Thienemanniola* and *Constempellina* were separated in the combined training set according to their contemporary occurrence described in species checklists (Paasivirta 2014, Sæther and Spies 2013). In some cases (including *Ablabesmyia*, *Dicrotendipes* and *Microtendipes*), species type-level identification was scaled to genus-level.

2.3. Statistical analyses

Taxon-specific mean July temperature optima in the merged dataset were estimated using Weighted Averaging (WA) with log10 transformed species data in the program C2 version 1.7.2 (Juggins 2007). Generalized Linear Modeling (GLM) was used to assess taxa that significantly ($p \leq 0.05$) respond to mean July air temperature. The GLMs were run using Poisson distribution in the program Past3 (Hammer 2001). Detrended Correspondence Analysis (DCA) was used to assess the gradient lengths of the first two DCA axis for selection of the most suitable methods for further analyses. For linearly distributed data with short gradient lengths, Principal Component Analysis (PCA) and redundancy analysis (RDA) are the most suitable methods (Šmilauer & Lepš 2014). The primary PCA axis scores were compared with site-specific temperatures using Pearson Product-moment correlation coefficient (R), coefficient of determination (R^2) and the level of statistical

150 significance ($p < 0.05$) to verify that the communities are responding to temperature. In addition,
151 RDA with forward-selected environmental variables and 999 unrestricted permutations was used to
152 partial out the significance of temperature, depth and pH (variables available from all datasets) on
153 the chironomid assemblages in the joint dataset. The DCA, PCA and RDA were performed with
154 log10 transformed species data using the CANOCO 5 program (Šmilauer & Lepš 2014).
155 The combined East European chironomid-based calibration model of mean July air
156 temperature was developed using the Weighted Averaging - Partial Least Squares technique (WA-
157 PLS), also with log10 transformed species data. The number of useful regression calibration
158 components was assessed using *t*-test (significance level 0.05). Model performance was evaluated
159 using jackknife cross-validation and subsequent coefficient of determination (R^2_{Jack}), root mean
160 squared error of prediction (RMSEP) and mean and maximum biases. The model was constructed
161 using the program C2 version 1.7.2 (Juggins 2007), in which also other common model types were
162 initially tested.
163 The model was verified against instrumentally measured (meteorological) temperatures
164 available since the 1830s in the shortcore sediment record from Nurmijärvi. The chironomid-
165 inferred temperatures were tested against the observational data by applying R, R^2 and $p < 0.05$.
166 Sample-specific modeling errors (estimated standard error of prediction = eSEP) were determined
167 using bootstrapping cross-validation with 999 iterations. The model was also run to reconstruct
168 temperatures in the Żabieniec long-core sediment record. LOESS smoothing was used to depict
169 general trends using a span of 0.2. To test whether the Żabieniec reconstruction corresponded to the
170 primary chironomid community variability, the temperatures were compared against the PCA axis 1
171 scores using Pearson product-moment correlation coefficient and the associated level of statistical
172 significance. Using the modern analogue technique, the cut-level of the 5^{th} percentile of all squared-
173 chord distances in the modern calibration data was determined. These distances were then compared
174 to the distance between each fossil assemblage and its most similar assemblage in the modern data

175 set and used to define 'no close' analogues. The reconstruction was compared with previous
176 chironomid-based reconstructions from the focal core using the Norwegian (Brooks & Birks 2001,
177 unpubl.), Russian (Self et al. 2011) and Swiss (Heiri & Lotter 2005, Bigler et al. 2006, von Gunten
178 et al. 2008) calibration models. In addition, the reconstructed general local trends in temperature
179 were compared with an ice-core temperature record (site-specific calibrations using ice-isotopic
180 ratios, borehole temperatures and gas-isotopic ratios) from Greenland (GISP2, Cuffey & Clow
181 1997, Alley 2000) representing hemispheric climate development.
182
183 **3. RESULTS**
184
185 After merging the Finnish and Polish chironomid training sets, 142 taxa were encountered
186 from the 212 calibration sites (Fig. 2). *Psectrocladius sordidellus*-type occurred in 86 sites,
187 *Polypedilum nubeculosum*-type in 80 sites and *Dicrotendipes* and *Procladius* in 79 sites.
188 *Limnophyes* reached the maximum relative abundance (75%) in a single site. *Lauterborniella*
189 *agrayloides* (6.7%), *Ablabesmyia* (6.5%) and *Paratendipes nudisquama*-type (5.4%) had the
190 highest mean abundances in the combined dataset.
191 The taxa with coldest temperature optima (12.5-13.1 °C) included *Heterotrissocladius*
192 *maeaeri*-type, *Psectrocladius calcaratus*-type and *Zalutschia* type B, whereas the taxa having
193 warmest optima included *Polypedilum sordens*-type, *Glyptotendipes barbipes*-type and *Labrundinia*
194 *longipalpis* (18.8-18.9 °C) (Fig. 3). Taxa with intermediate temperature optima (16-17 °C) and wide
195 tolerances included *Paratanytarsus penicillatus*-type, *Dicrotendipes*, *Procladius* and *Chironomus*
196 *anthracinus*-type. Of the most common taxa (N > 5), only *Dicrotendipes* did not respond
197 statistically significantly to the temperature gradient (Fig. 3). For most taxa, the GLMs showed
198 significant linear fit, however, significant nonlinear distribution was found in some taxa with
199 intermediate temperature optima, including *Tanytarsus chinyensis*-type 1, *Natarsia Punctata*-type,

200 *Corynoneura lobata*-type, *Smittia* and *Endochironomus impar*-type. *Paratanytarsus penicillatus*-
201 type was the only taxon with bimodal distribution, with highest abundances at the both ends of the
202 temperature gradient.

203 The initial DCA indicated a gradient length of 2.8 SD for the surface sediment chironomid
204 assemblages. Hence, owing to the linear nature of the data, PCA was recommended for ordination
205 analysis (Šmilauer and Lepš, 2014). Subsequently, the PCA axis 1 showed an eigenvalue of 0.1974
206 and the axis 2 an eigenvalue of 0.0659. The first axis explained 19.7% and the second 6.6% of the
207 total variance. The first four axes explained 36.1% of the variance in total. In the ordination (Fig. 4),
208 the samples along the primary PCA axis were arranged according to the site-specific mean July air
209 temperatures, with Polish sites (warm) having negative scores and Finnish sites (cold) positive
210 scores (Fig. 4a). The warm and cold indicator taxa identified with the PCA ordination (Fig. 4b)
211 were the same as indicated with the WA optima and GLMs (Fig. 3). The PCA axis 1 scores of the
212 samples were strongly correlated with the site-specific temperatures having an R of 0.91, R^2 of 0.82
213 and $p < 0.001$. The RDA results showed that temperature was the most important variable in
214 explaining chironomid distribution of the examined variables. Of variation explained by the
215 examined variables (15.4%), temperature explained 78.8%, pH 13.7% and depth 7.5% (Table 2).
216 Consequently, temperature had clearly the highest λ_1:λ_2 ratio (1.061) that justified the construction
217 of the chironomid-based temperature model.

218 Compared to other model types, WA-PLS had the best performance statistics with
219 respect to its R^2_{Jack} and RMSEP (Table 3). The developed WA-PLS model for mean July air
220 temperature had an R^2_{Jack} of 0.88, RMSEP of 0.88 °C and mean and maximum biases of -0.02 and
221 0.79 °C, respectively (Table 4). Addition of the second regression calibration component reduced
222 the RMSEP by 8.8% (randomization *t*-test significance 0.004). The 1:1 relationship between the
223 inferred and observed temperatures in the model illustrated that the combined calibration set has a

well-structured continuum in its temperature range with relatively even distribution of samples (Fig. 5a).

The test of the developed model on the clastic-biogenic varve record from Lake Nurmijärvi showed similar trends between the chironomid-inferred and meteorologically observed temperatures over the instrumental period. In both inferred and observed records (Fig. 6a), the temperatures remained low during the 19th century with increased temperatures at the 1930s. Following intermediate summer temperatures, the climate began to warm in the 1990s and record highest temperatures synchronously occurred during the 21th century. The correlation between the observed and inferred temperatures at the test site was statistically significant (R = 0.72, R^2 = 0.52, $R_{corrected}$ = 0.51, $p < 0.001$), although in several samples the temperature difference was larger than the sample-specific error estimate (Fig. 6b).

In the long-core reconstruction, samples 1608-1181 cm (older than 15,000 cal yr BP) had poor modern analogues according to the MAT suggesting that the early part of the sequence may not be reliably reconstructed. Nonetheless, the reconstructed values correlated with the primary PCA axis scores (R=0.50, p<0.001) indicating that chironomids do respond to the reconstructed variable in the sediment profile. The chironomid-inferred temperature trends using the East European model were rather similar to those reconstructed using the Norwegian, Russian and Swiss models (Fig. 7). However, the new model reconstructed higher temperatures for the initial part of the sediment record (1600-1500 cm, no age estimate), where poor modern analogues occurred. In all, the East European model was most similar with the reconstruction derived using the Russian model, whereas larger differences existed when compared with the results using the Norwegian and Swiss models. In addition to the early part of the record, the East European model reconstructed high temperatures between 16,000-12,000 cal yr BP and during the past ~1000 yr. Based on the new model, the most distinct cold events occurred between 1400-1300 cm (ending at ~17,000-16,000 cal yr BP) and 2000-1000 cal yr BP. However, the latter cold event occurs in samples with

low chironomid count sums and presence of semiterrestrial taxa (see Płóciennik et al. 2011 for details). When compared with the GISP2 record, the warm period at 15,000 cal yr BP and the following cooling is well represented. The rapid temperature rise during the early Holocene suggested by the GISP data and the late Holocene cooling trend in the current record suggest differences between the regional and global records.

4. DISCUSSION

4. 1. Training set

Combination of the Finnish and Polish chironomid datasets yielded a training set with a temperature gradient of 8.8 °C (11.3-20.1 °C) enabling wider usability with respect to paleoclimate reconstructions. The cold indicators (Figs 2, 3, 4b) in the combined dataset, such as *Heterotrissocladius maeaeri*-type, *H. grimshawi*-type, *Psectrocladius calcaratus*-type, *Sergentia coracina*-type, *Micropsectra insignilobus*-type and *Tanytarsus lugens*-type are commonly found also in the cold lakes of other training sets from Eurasia (Heiri et al. 2011, Self et al. 2011). Similarly, the warm preferring chironomids, such as *Polypedilum sordens*-type, *Glyptotendipes barbipes*-type, *G. pallens*-type and *Endochironomus albipennis*-type are typical warm indicators in various other datasets (Heiri et al. 2003, Self et al. 2011). These warm taxa also appear to be more common in meso-eutrophic lakes, whereas the cold taxa are more often found in oligotrophic sites (Brooks et al. 2001, Brodersen & Quinlan 2006, Luoto 2011). This occurrence pattern has been previously documented (Eggermont & Heiri 2012) and is for large part related to the fact that warm lakes are often more productive and human influenced compared to the naturally oligotrophic cold lakes. In addition, the results showed that *Paratanytarsus penicillatus*-type, *Dicrotendipes*, *Procladius* and *Chironomus anthracinus*-type are eurythermic taxa having large temperature

tolerances (Figs 3, 4b) that has also been described in various other datasets (Larocque et al. 2006, Fortin et al. 2015, Nazarova et al. 2015). These taxa aggregate several species that is probably one of the reasons for their broad tolerance values. Of the most common taxa (Figs 2, 3), only *Dicrotendipes* did not have a statistically significant relationship with temperature and *P. penicillatus*-type was the only one having a bimodal distribution. These factors inevitably influence their use as temperature indicators. Although the general temperature indication of the taxa is in most part similar to the other training sets, there are significant differences in the values of the taxa-specific temperature optima that are related to the temperature gradients of the respective datasets. These regional differences in optima will become significant when selecting the training set to be used in a downcore, seriously affecting the reconstructed quantitative values (Engels et al. 2014, Fortin et al. 2015).

The PCA indicated a humped distribution of the samples in the ordination space (Fig. 4). The samples were clearly distributed along the primary PCA axis according to their site-specific temperatures that was also verified by the high correlation ($R = 0.91$, $R^2 = 0.82$, $p < 0.001$) between the PCA 1 scores and observed temperatures at the sites. Although the ordination plot illustrates that the secondary gradient also has influence on the assemblages, the PCA axis 2 explained only 6.6% of the total variance. In addition, the RDA results (Table 2) clearly indicated that temperature is the most significant variable explaining chironomid distribution among the mutually measured variables in the Finnish and Polish datasets. Importantly, water depth, which has been found significant in explaining intralake chironomid distributions in Finland (Luoto 2010) and elsewhere (Kurek & Cwynar 2009, Engels et al. 2012, Luoto 2012a, 2012b), explained only a minor share of the chironomid community compositions. Therefore, these results demonstrate that the chironomid assemblages closely respond to mean July air temperature in the combined dataset, and consequently justify the development of the East European chironomid-based temperature model. The primary response of chironomids to temperature has been clearly evidenced in a bulk of

distributional studies (Larocque & Hall 2003, Nyman et al. 2005, Brooks et al. 2012) and their biological response to temperature is also evident (Rossaro 1991, Eggermont & Heiri 2012). Nonetheless, detecting the potential influence of secondary environmental gradients, such as water depth, nutrients and DOC, on chironomid-based paleotemperature reconstructions remains important, especially since their significance may vary in time (Nyman et al. 2008, Shala et al. 2014, Medeiros et al. 2015).

4.2. Calibration model

The developed temperature calibration model used WA-PLS technique, which outperformed the other tested model types (Table 3). Typical for chironomid-temperature calibration models (Heiri et al. 2011), the use of two WA-PLS components was statistically justified. The model's statistical performance (Fig. 5), measured in R^2_{Jack}, was comparable with other chironomid-based temperature models (Heiri et al. 2011, Holmes et al. 2011) but in its RMSEP (0.88 °C, 10% of calibration set gradient) it outperformed several of the other models, many of them having RMSEPs >1 °C (Barley et al. 2006, Porinchu et al. 2009, Nazarova et al. 2011). Compared to the new East European model, the original latitudinal Finnish temperature model had lower R^2_{Jack} (0.78) but also lower RMSEP (0.72 °C, 12.4% of calibration set gradient) (Table 4). However, since RMSEP is inherently influenced by the gradient length of the examined variable, it may be more useful to compare the RMSEPs in relation to the temperature gradients. In this sense, the RMSEP is more favorable in the combined model.

The combination of the Finnish and Polish datasets resulted as a consistent continuum in the model's predictive abilities, as the Polish sites increased the temperature gradient of the model towards warmer temperatures (Fig. 5a). Longer environmental gradients will help in situations where past climate conditions approach the specific dataset's temperature limits (Birks et al. 2003).

Slight distortions at both ends of the temperature gradient were observed (Fig. 5b) that is inherent in WA-PLS models (Heiri & Lotter 2010). This distortion, i.e. edge-effect, causes underestimation of warm temperatures and overestimation of cold temperatures, and hence potentially smoothen reconstructions.

4.3. Reconstructions

The best means to verify environmental reconstructions is to compare them with instrumentally measured data (Larocque et al. 2009, Larocque-Tobler et al. 2015). Our test site, Lake Nurmijärvi with sediments constituting of clastic biogenic varves, is located in southcentral Finland, close to the warm end of the temperature gradient of the original Finnish training set (Fig. 1). The reconstruction results showed that the East European model has the ability to accurately predict downcore temperatures, as it well-depicted the cold temperatures of the 19th century, the increased temperatures of the 1930s and the rapid warming that began in the 1980s (Fig. 6). The mean difference in the inferred values compared to the observed was only 0.3 °C but the largest overestimation was 3.0 °C and underestimation 2.7 °C. The biased values are most likely related to lags in chironomid response times, since many taxa have long life cycles and their dispersal, although fast compared to many other biological proxies (Wu et al. 2015), can take up to seven years (Pinder 1986). The correlation between reconstructed and observed temperatures was higher than in the previous study where the latitudinal Finnish model was used (Luoto & Ojala 2017), clearly suggesting that the new model has better prediction accuracy and reliability compared to the original model.

Since the model had solid performance statistics and it was able to reconstruct similar temperatures with the observational record in southern Finland, we also applied it to a long-core taken from the Żabieniec paleolake in Poland. Importantly, the chironomid-inferred values showed

significant correlation with the primary ordination axis scores verifying that chironomids respond to temperature in the Żabieniec record. The previous study from the site demonstrated that chironomid-based temperature models from outside the geographical area reconstructed partly differing temperatures (Płóciennik et al. 2011). The present results showed that the developed East European model reconstructed temperatures that mostly resemble those reconstructed using the Russian model (Self et al. 2011) (Fig. 7), whereas distinct differences were apparent when compared with the Swiss (Heiri & Lotter 2005) and Norwegian models (Brooks & Birks 2001) (Fig. 7). These differences include very low temperatures in the initial part of the record and the absence of the late Holocene cooling trend (Wanner et al. 2015). The early phase of the record may be connected with the warm Kamion phase previously described from Poland (Manikowska 1995), however, this remains uncertain due to lack of detailed chronological control in the bottom part of the Żabieniec sediment sequence. Although the present interpretations are based solely on mean July air temperature and there is no data on winter conditions or vegetational season length, it may still be speculated that the climate conditions during the early phase of the record were glacial, but because of high continentality summers were warm as in Siberia (Klimanov 1997). This interpretation would be logical also considering that the East European and Russian models produce similar warm temperatures for this phase differing from those derived using the Swiss and Norwegian models (Fig. 6).

It is possible that the late Glacial temperatures could have been colder in Żabieniec than the lowest temperatures represented by the calibration sites. However, the reconstructed temperatures are not close the limits of the model (11 °C) but remain at >14 °C (Fig. 7). If the actual temperatures would have been colder and the chironomid taxa would have consisted solely of taxa with coldest temperature preferences, the WA-PLS model would have the potential to extrapolate beyond the cold gradient end (Velle et al. 2011). This was not the case in the present data, where late Glacial sequences consisted of taxa with intermediate temperature optima, such as

374 *Procladius* and *Tanytarsus pallidicornis*-type (Fig. 7). These taxa are also known to have wider
375 trophic tolerances (Brodersen & Quinlan 2006), which could reflect elevated nutrient condition
376 during the early part of the sediment profile. In contrast, the Norwegian, Russian and Swiss
377 calibration models all reconstruct consistently colder late Glacial temperatures than the East
378 European model. This is probably related to the compared calibration models having generally
379 colder lakes among the training set sites, and hence, the new model would benefit from inclusion on
380 even colder sites than it currently has. Despite the extrapolation capabilities of the WA-PLS
381 method, it is clear that the East European model can be reliable only within its temperature gradient
382 (11-20 °C), with decreasing reliability towards the gradient ends. Consequently, the coldest and
383 warmest episodes in long sediment records, such as the Żabieniec record, should be considered
384 cautiously when observing the reconstructed values, although at the same time the trends may be
385 realistic. It is also noteworthy that the late Glacial chironomid assemblages had poor modern
386 analogues in the calibration set that decreases the reliability of the new reconstruction during this
387 early phase of the record.
388 Similar to the other chironomid-based reconstructions, the new reconstruction did not
389 depict significant temperature drop during the cold Younger Dryas period. There are also no distinct
390 changes in the taxonomic composition at this time (Płóciennik et al. 2011, Fig. 7) that could
391 indicate other driving factors that would potentially reduce the temperature signal. This period was
392 unusually cold in Scandinavia (Brooks & Birks 2000, Wohlfarth et al. 2018) but in several studies
393 from Poland (Zawiska et al. 2015, Pawłowski et al. 2015, 2016a, 2016b) and Central Europe
394 (Larocque-Tobler et al. 2010), the summer temperature drop during the Younger Dryas has been
395 relatively muted compared to the British Isles, the Baltic region and the northern parts of the
396 continent (Heiri et al. 2014). Therefore, the present results are consistent with the previous studies
397 from Poland showing intra-European differences. Compared to the other chironomid-based
398 reconstructions from Żabieniec, the East European model reconstructs similar 16-17 °C

399 temperatures, with the exception of the Norwegian model, which indicates slightly lower
400 temperatures (Fig. 7).

401 Compared to hemispheric temperatures reflected by the GISP2 ice core record (Cuffey &
402 Clow 1997; Alley 2000), the current reconstruction does not suggest similar increase in early
403 Holocene temperatures (Fig. 7). The rapid early Holocene temperature increase has been described
404 from several lake sediment records from northern Europe (Brooks & Birks 2000, Engels et al. 2014,
405 Luoto et al. 2014, Shala et al. 2017, Helmens et al. 2018) and the European Alps (Samartin et al.
406 2012). The increase in *Lauterborniella* between 10,000 and 8000 cal yr BP can be related to
407 nutrient conditions, since in addition to high temperature optimum, it is known to thrive in more
408 nutrient-enriched lakes (Brooks et al. 2007). However, the warming associated with the increase in
409 *Lauterborniella* is consistent with the increased temperatures in the GISP2 record following the
410 cold early Holocene. The late Holocene cooling trend is not apparent in the GISP2 record, although
411 clearly seen from the present results and several other records from Poland (Zawiska et al. 2015,
412 Pawłowski et al. 2015, 2016b) suggesting regional deviation from hemispheric temperatures.
413 Nonetheless, it should be noted that the temperature decrease reconstructed from Żabieniec between
414 2000 and 1000 cal yr BP is not reliable owing to dominance of semiterrestrial chironomid taxa and
415 low count sums (Płóciennik et al. 2011). Compared to the reconstructions performed using the other
416 chironomid-based models and the GISP2 record, the temperatures reconstructed using the East
417 European model showed a distinct warming during the past 1000 yr, with a short-lived drop in
418 temperatures during the Little Ice Age. In general, the reconstruction of the Holocene temperatures
419 in Żabieniec paleolake closely resembles those from elsewhere in Europe (Davis et al. 2003, Luoto
420 et al. 2010, Engels et al. 2014) combined with distinct local features (Zawiska et al. 2015,
421 Pawłowski et al. 2015, 2016b), hence signifying the reliability of the reconstruction.
422

423 **5. CONCLUSIONS**

Merging the Finnish and Polish chironomid-based training sets resulted as a valid calibration model for mean July air temperature with an extended temperature gradient and improved applicability. The temperature indicators were similar to what has been found in previous studies, however, the numerical optima more accurately adjusted for the study area. The statistical tests showed that chironomids were responding most strongly to temperature, hence enabling construction of the enhanced model. Compared to previous chironomid-temperature models in general, the new East European model has solid performance statistics.

The model validation in a Finnish annually laminated lake sediment record, covering the observational temperature period beginning from the 1830s, showed that the model better predicts paleotemperatures compared to the original Finnish model. Since the inferred temperatures correlated strongly with the instrumental record, the model can be considered solid with respect to its predictive abilities and applicability in downcore profiles from Eastern Europe. The reconstructed temperatures using the East European model in the long-core from the Polish paleolake Żabieniec, covering the past ~20,000 yr, were more similar to temperatures reconstructed using the Russian chironomid-based model than the ones reconstructed using the Swiss and Norwegian models. The reconstructed temperature trends were comparable to previous studies from Poland but significantly different from hemispheric paleotemperature estimates signifying the importance of local reconstructions in understanding past climate oscillations.

Although the model is designed for Finnish and Polish sites as a preset, it can be useful in other areas of Eastern Europe as well. In the future, the East European model can be further developed especially by including additional calibration sites from the Baltic Countries that would promote stability of the model. In all, the present results demonstrate the usability and sensitivity of fossil chironomids as quantitative paleoclimate indicators.

Acknowledgements. This study was funded by the Emil Aaltonen Foundation (grants 160156, 170161 and 180151), grant of Polish Ministry of Science and Higher Education (2 P04E 02228), SYNTHESYS EU grant for Żabieniec chironomid sequence studies, Polish Geological Institute – National Research Institute grants (61.3608.1401.00.0 and 65-3608-1401-00-0) and SYNTHESYS European Community Research Infrastructure Action under the FP7 "Capacities" Program" for Polish Chironomidae calibration set. Support for mobility by the EU Climate-KIC's Pioneers into Practice programme is deeply appreciated. We are grateful for the three journal reviewers for their constructive comments and help to improve the manuscript.

LITERATURE CITED

Alley RB (2000) The Younger Dryas cold interval as viewed from central Greenland. Quat Sci Rev 19:213–226

Barley EM, Walker IR, Kurek J, Cwynar LC, Mathewes RW, Gajewski K, Finney BP (2006) A northwest North American training set: distribution of freshwater midges in relation to air temperature and lake depth. J Paleolimnol 36:295–314

Bigler C, Heiri O, Krskova R, Lotter AF, Sturm M (2006) Distribution of diatoms, chironomids and cladocerans in surface sediments of thirty mountain lakes in southeastern Switzerland. Aquat Sci 68:154–171

Birks HJB, Mackay A, Battarbee RW, Birks J, Oldfield F (2003) Quantitative palaeoenvironmental reconstructions from Holocene biological data. Global change in the Holocene pp. 107–123

474 Brodersen KP, Quinlan R (2006) Midges as palaeoindicators of lake productivity, eutrophication
475 and hypolimnetic oxygen. Quat Sci Rev 25:1995–2012
476
477 Brooks SJ (2006) Fossil midges (Diptera: Chironomidae) as palaeoclimatic indicators for the
478 Eurasian region. Quat Sci Rev 25:1894–1910
479
480 Brooks SJ, Birks HJB (2001) Chironomid-inferred air temperatures from Lateglacial and Holocene
481 sites in north-west Europe: progress and problems. Quat Sci Rev 20:1723–1741
482
483 Brooks SJ, Axford Y, Heiri O, Langdon PG, Larocque-Tobler I (2012) Chironomids can be reliable
484 proxies for Holocene temperatures. A comment on Velle et al. (2010). Holocene 22:1495–1500
485
486 Brooks SJ, Langdon PG, Heiri O (2007) The identification and use of Palaearctic Chironomidae
487 larvae in palaeoecology. QRA Technical Guide No. 10. Quaternary Research Association, London.,
488 276 pp
489
490 Brooks SJ, Bennion H, Birks HJB (2001) Tracing lake trophic history with a chironomid–total
491 phosphorus inference model. Freshw Biol 46:513–533
492
493 Cuffey KM, Clow GD (1997) Temperature, accumulation, and ice sheet elevation in central
494 Greenland through the last deglacial transition. J Geophys Res 102:26383–26396
495
496 Davis BA, Brewer S, Stevenson AC, Guiot J (2003) The temperature of Europe during the
497 Holocene reconstructed from pollen data. Quat Sci Rev 22:1701–1716
498

499 Eggermont H, Heiri O (2012) The chironomid-temperature relationship: expression in nature and
500 palaeoenvironmental implications. Biol Rev 87:430–456
501
502 Engels S, Self AE, Luoto TP, Brooks SJ, Helmens KF (2014) A comparison of three Eurasian
503 chironomid-climate calibration datasets on a W-E continentality gradient and the implications for
504 quantitative temperature reconstructions. J Paleolimnol 51:529–547
505
506 Engels S, Cwynar LC, Rees AB, Shuman BN (2012) Chironomid-based water depth
507 reconstructions: an independent evaluation of site-specific and local inference models. J
508 Paleolimnol 48:693–709
509
510 Fortin MC, Medeiros AS, Gajewski K, Barley EM, Larocque-Tobler I, Porinchu DF, Wilson SE
511 (2015) Chironomid-environment relations in northern North America. J Paleolimnol 54:223–237
512
513 Hammer Ø, Harper DAT, Ryan PD (2001) PAST: Paleontological statistics software package for
514 education and data analysis. Palaeontol Electron 4:1–9
515
516 Heiri O, Lotter AF (2010) How does taxonomic resolution affect chironomid-based temperature
517 reconstruction? J Paleolimnol 44:589–601
518
519 Heiri O, Lotter AF (2005) Holocene and Late Glacial summer temperature in the Swiss Alps based
520 on fossil assemblages of aquatic organisms: a review. Boreas 34:506–516
521

522 Heiri O, Brooks SJ, Birks HJB, Lotter AF (2011) A 274-lake calibration data-set and inference
523 model for chironomid-based summer air temperature reconstruction in Europe. Quat Sci Rev
524 30:3445–3456
525
526 Heiri O, Lotter AF, Hausmann S, Kienast F (2003) A chironomid-based Holocene summer air
527 temperature reconstruction from the Swiss Alps. Holocene 13:477–484
528
529 Heiri O et al. (2014) Validation of climate model-inferred regional temperature change for late-
530 glacial Europe. Nat Com 5:4914
531
532 Helmens KF, Katrantsiotis C, Salonen JS, Shala S, Bos JAA, Engels S, Kuosmanen N, Luoto TP,
533 Väliranta M, Luoto M, Ojala AEK, Risberg J, Weckström J (2018) Warm summers and rich biotic
534 communities during N-Hemisphere deglaciation. Global Planet Change 167:61–73
535
536 Holmes N, Langdon PG, Caseldine C, Brooks SJ, Birks HJB (2011) Merging chironomid training
537 sets: implications for palaeoclimate reconstructions. Quat Sci Rev 30:2793–2804
538
539 Ilyashuk EA, Koinig KA, Heiri O, Ilyashuk BP, Psenner R (2011) Holocene temperature variations
540 at a high-altitude site in the Eastern Alps: a chironomid record from Schwarzsee ob Sölden, Austria.
541 Quat Sci Rev 30:176–191
542
543 Juggins S (2007) C2: Software for ecological and palaeoecological data analysis and visualisation
544 (user guide version 1.5). Newcastle upon Tyne, Newcastle University
545

546 Klimanov VA (1997) Late glacial climate in northern Eurasia: the last climatic cycle. Quat Int
547 41:141–152
548
549 Kurek J, Cwynar LC (2009) Effects of within-lake gradients on the distribution of fossil
550 chironomids from maar lakes in western Alaska: implications for environmental reconstructions.
551 Hydrobiologia 62:337–52
552
553 Lamentowicz M., Balwierz Z, Forysiak J, Płóciennik M, Kittel P, Kloss M, Twardy J, Żurek S,
554 Pawlyta J (2009) Multiproxy study of anthropogenic and climatic changes in the last two millennia
555 from a small mire in central Poland. Hydrobiologia 631:213–230
556
557 Larocque I, Hall RI (2003) Chironomids as quantitative indicators of mean July air temperature:
558 validation by comparison with century-long meteorological records from northern Sweden. J
559 Paleolimnol 29:475–493
560
561 Larocque I, Pienitz R, Rolland N (2006) Factors influencing the distribution of chironomids in lakes
562 distributed along a latitudinal gradient in northwestern Quebec, Canada. Can J Fish Aquat Sci
563 63:1286–1297
564
565 Larocque-Tobler I, Filipiak J, Tylmann W, Bonk A, Grosjean M (2015) Comparison between
566 chironomid-inferred mean-August temperature from varved Lake Żabińskie (Poland) and
567 instrumental data since 1896 AD. Quat Sci Rev 111:35–50
568

569 Larocque I, Grosjean M, Heiri O, Bigler C, Blass A (2009) Comparison between chironomid-
570 inferred July temperatures and meteorological data AD 1850–2001 from varved Lake Silvaplana,
571 Switzerland. J Paleolimnol 41:329–342
572
573 Larocque-Tobler I, Heiri O, Wehrli M (2010) Late Glacial and Holocene temperature changes at
574 Egelsee, Switzerland, reconstructed using subfossil chironomids. J Paleolimnol 43:649–666
575
576 Linderholm HW et al. (2018) Arctic hydroclimate variability during the last 2000 years – current
577 understanding and research challenges. Clim Past 14:1–42
578
579 Luoto TP (2012a) Intra-lake patterns of aquatic insect and mite remains. J Paleolimnol 47:141–157
580
581 Luoto TP (2012b) Spatial uniformity in depth optima of midges: evidence from sedimentary
582 archives of shallow Alpine and boreal lakes. J Limnol 71:228–232
583
584 Luoto TP (2011) The relationship between water quality and chironomid distribution in Finland – A
585 new assemblage-based tool for assessments of long-term nutrient dynamics. Ecol Indic 11:255–262
586
587 Luoto TP (2010) Hydrological change in lakes inferred from midge assemblages through use of an
588 intralake calibration set. Ecol Monogr 80:303–329
589
590 Luoto TP (2009) Subfossil Chironomidae (Insecta: Diptera) along a latitudinal gradient in Finland:
591 development of a new temperature inference model. J Quat Sci 24:150–158
592

593 Luoto TP, Ojala AEK (2017) Meteorological validation of chironomids as a paleotemperature
594 proxy using varved lake sediments. Holocene 27:870–878
595
596 Luoto TP, Ojala AEK, Arppe L, Brooks SJ, Kurki E, Oksman M, Wooller MJ, Zajączkowski M
597 (2018) Synchronized proxy-based temperature reconstructions reveal mid- to late Holocene climate
598 oscillations in High Arctic Svalbard. J Quat Sci 33:93–99
599
600 Luoto TP, Rantala MV, Galkin A, Rautio M, Nevalainen L (2016) Environmental determinants of
601 chironomid communities in remote northern lakes across the treeline – Implications for climate
602 change assessments. Ecol Indic 61:991–999
603
604 Luoto TP, Kaukolehto M, Weckström J, Korhola A, Väliranta M (2014) New evidence of warm
605 early-Holocene summers in subarctic Finland based on an enhanced regional chironomid-based
606 temperature calibration model. Quat Res 81:50–62
607
608 Luoto TP, Kultti S, Nevalainen L, Sarmaja-Korjonen K (2010) Temperature and effective moisture
609 variability in southern Finland during the Holocene quantified with midge-based calibration models.
610 J Quat Sci 25:1317–1326
611
612 Manikowska B (1995) Aeolian activity differentiation in the area of Poland during the period 20-8
613 ka BP. Biuletyn Peryglacjalny 34:127–165
614
615 McCarroll D (2015) 'Study the past, if you would divine the future': a retrospective on measuring
616 and understanding Quaternary climate change. J Quat Sci 30:154–187
617

618 Medeiros AS, Gajewski K, Porinchu DF, Vermaire JC, Wolfe BB (2015) Detecting the influence of
619 secondary environmental gradients on chironomid-inferred paleotemperature reconstructions in
620 northern North America. Quat Sci Rev 124:265–274
621
622 Nazarova L, Self AE, Brooks SJ, van Hardenbroek M, Herzschuh U, Diekmann B (2015) Northern
623 Russian chironomid-based modern summer temperature data set and inference models. Global
624 Planet Change 134:10–25
625
626 Nazarova L, Herzschuh U, Wetterich S, Kumke T, Pestryakova L (2011) Chironomid-based
627 inference models for estimating mean July air temperature and water depth from lakes in Yakutia,
628 northeastern Russia. J Paleolimnol 45:57–71
629
630 Nyman M, Weckström J, Korhola A (2008) Chironomid response to environmental drivers during
631 the Holocene in a shallow treeline lake in northwestern Fennoscandia. Holocene 18:215–227
632
633 Nyman M, Korhola A, Brooks SJ (2005) The distribution and diversity of Chironomidae (Insecta:
634 Diptera) in western Finnish Lapland, with special emphasis on shallow lakes. Global Ecol Biogeogr
635 14:137–153
636
637 Ojala AEK, Mattila J, Virtasalo J, Kuva J, Luoto TP (2018) Seismic deformation of varved
638 sediments in southern Fennoscandia at 7400 cal BP. Tectonophysics 744:58-71
639
640 Ojala AEK, Luoto TP, Virtasalo JJ (2017) Establishing a high-resolution surface sediment
641 chronology with multiple dating methods – Testing ^{137}Cs determination with Nurmijärvi clastic-
642 biogenic varves. Quat Geochronol 37:32–41

643

644 Pawłowski D, Borówka RK, Kowalewski G, Luoto TP, Milecka K, Nevalainen L, Okupny D,
645 Płóciennik M, Woszczyk M, Tomkowiak J, Zieliński T (2016a) The response of flood-plain
646 ecosystems to the Late Glacial and Early Holocene hydrological changes: A case study from a small
647 Central European river valley. Catena 147:411–428

648

649 Pawłowski D, Borówka RK, Kowalewski G, Luoto TP, Milecka K, Nevalainen L, Okupny D,
650 Zieliński T, Tomkowiak J (2016b) Late Weichselian and Holocene record of the
651 paleoenvironmental changes in a small river valley in Central Poland. Quat Sci Rev 135:24–40

652

653 Pawłowski D, Płóciennik M, Brooks SJ, Luoto TP, Milecka K, Nevalainen L, Peyron O, Self A,
654 Zieliński T (2015) A multiproxy study of Younger Dryas and Early Holocene climatic conditions
655 from the Grabia River palaeo-oxbow lake (central Poland). Palaeogeogr Palaeoclimatol Palaeoecol
656 438:34–50

657

658 Paasivirta L (2014) Checklist of the family Chironomidae (Diptera) of Finland. ZooKeys 441:63–90

659

660 Pinder LCV (1986) Biology of freshwater Chironomidae. Annu Rev Entomol 31:1–23

661

662 Płóciennik M, Self A, Birks HJB, Brooks SJ (2011) Chironomidae (Insecta: Diptera) succession in
663 Żabieniec bog and its palaeo-lake (central Poland) through the Late Weichselian and Holocene.
664 Palaeogeogr Palaeoclimatol Palaeoecol 307:150–167

665

666 Porinchu D, Rolland N, Moser K (2009) Development of a chironomid-based air temperature
667 inference model for the central Canadian Arctic. J Paleolimnol 41:349–368

668

669 Rantala MV, Luoto TP, Nevalainen L (2016) Temperature controls organic carbon sequestration in
670 a subarctic lake. Sci Rep 6:34780

671

672 Rossaro B (1991) Chironomids and water temperature. Aquat Insects 13:87–98

673

674 Sæther OA, Spies M (2013) Fauna Europaea: Chironomidae. Fauna Europaea: Diptera Nematocera.
675 Fauna Europaea version, 2.2

676

677 Samartin S, Heiri O, Vescovi E, Brooks SJ, Tinner W (2012) Lateglacial and early Holocene
678 summer temperatures in the southern Swiss Alps reconstructed using fossil chironomids. J Quat Sci
679 27:279–289

680

681 Self A, Brooks SJ, Birks HJB, Nazarova LB, Porinchu D, Odland A, Yang H, Jones VJ (2011) The
682 influence of temperature and continentality on modern chironomid assemblages in high-latitude
683 Eurasian lakes: development and application of new chironomid-based climate-inference models in
684 northern Russia. Quat Sci Rev 30:1122–1141

685

686 Shala S, Helmens KF, Luoto TP, Salonen JS, Väliranta M, Weckström J (2017) Comparison of
687 quantitative Holocene temperature reconstructions using multiple proxies from a northern boreal
688 lake. Holocene 27:1745–1755

689

690 Shala S, Helmens KF, Luoto TP, Väliranta M, Weckström J, Salonen JS, Kuhry P (2014)
691 Evaluating environmental drivers of Holocene changes in water chemistry and aquatic biota
692 composition at Lake Loitsana, NE Finland. J Paleolimnol 52:311–329

693

694 Šmilauer P, Lepš J (2014) Multivariate analysis of ecological data using CANOCO 5. Cambridge
695 University Press

696

697 Velle G, Kongshavn K, Birks HJB (2011) Minimizing the edge-effect in environmental
698 reconstructions by trimming the calibration set: Chironomid-inferred temperatures from
699 Spitsbergen. Holocene 21:417–430

700

701 von Gunten L, Heiri O, Bigler C, van Leeuwen J, Casty C, Lotter A., Sturm M (2008) Seasonal
702 temperatures for the past 400 years reconstructed from diatom and chironomid assemblages in a
703 high-altitude lake (Lej da la Tscheppa, Switzerland). J Paleolimnol 39:283–299

704

705 Wanner H, Mercolli L, Grosjean M, Ritz SP (2015) Holocene climate variability and change; a
706 data-based review. J Geol Soc 172, 254–263

707

708 Wohlfarth B, Luoto TP, Muschitiello F, Väliranta M, Björk S, Davies S, Kylander M, Ljung K,
709 Reimer P, Smittenberg RH (2018) Climate and environment in southwest Sweden 15.3 – 11.3 cal.
710 ka BP. Boreas 47:687-710

711

712 Wu D, Zhao X, Liang S, Zhou T, Huang K, Tang B, Zhao W (2015) Time-lag effects of global
713 vegetation responses to climate change. Glob Change Biol 21:3520–3531

714

715 Zawiska I, Słowiński M Correa-Metrio A, Obremska M, Luoto TP, Nevalainen L, Woszczyk M,
716 Milecka K (2015) The response of a shallow lake and its catchment to Late Glacial climate changes
717 – A case study from eastern Poland. Catena 126:1–10

Tables

Table 1. Characteristics of the study sites in the Finnish, Polish and the combined East European chironomid-based temperature datasets. Mean values are given in brackets.

	Finnish	Polish	Combined
Number of sites (N)	114	98	212
Number of taxa (N)	111	100	142
Latitude (°N)	60.13-69.55 (65.91)	49.19-54.68 (52.60)	49.19-69.55 (59.60)
Longitude (°E)	22.00-30.13 (26.55)	14.51-23.42 (18.42)	14.51-30.13 (22.69)
Elevation (m a.s.l.)	4-405 (157)	4-1624 (196)	4-1624 (174)
Temperature gradient (°C)	11.3-17.1 (14.4)	11.6-20.1 (18.6)	11.3-20.1 (16.4)
Sampling depth (m)	0.5-7.0 (2.3)	0.3-15.0 (8.8)	0.3-15.0 (5.7)
pH	4.6-8.4 (6.5)	5.1-9.8 (8.3)	4.6-9.8 (7.5)

Table 2. Redundancy analysis (RDA) results for the combined East European chironomid dataset. All examined variables together explain 15.4% of the total variance.

Variable	λ_1:λ_2	Contribution (%)	*F*	*p* ($p_{\text{bonferroni adjusted}}$)
Mean July air temperature	1.061	78.8	26.0	0.001 (0.003)
pH	0.563	13.7	4.6	0.001 (0.003)
Water depth	0.398	2.5	2.5	0.002 (0.006)

Table 3. Comparison of performance statistics using different model types (WA = weighted averaging, PLS = partial least squares) in the development of the East European chironomid-based calibration model. The model deemed most suitable for downcore reconstructions is marked with boldtype.

Calibration model type	Coefficient of determination (R^2_{jack})	Root mean squared error of prediction (RMSEP, °C)	Maximum bias (°C)	Reduction in RMSEP (%)
$WA_{inverse\ deshrinking}$	0.86	0.96	1.22	
$WA_{classical\ deshrinking}$	0.86	1.01	0.76	
$PLS_{component\ 1}$	0.84	1.04	1.51	
$PLS_{component2}$	0.86	0.96	0.93	7.99
$WA\text{-}PLS_{component1}$	0.86	0.97	1.24	
$WA\text{-}PLS_{component2}$	**0.88**	**0.88**	**0.79**	**8.78**

775 Table 4. Performance statistics of the developed East European chironomid-based temperature
776 calibration model compared with the original Finnish model (Luoto 2009).

	East European model	Finnish model
Number of sites (N)	212	82
Number of taxa (N)	142	110
Model type	WA-PLS, component 2	WA-PLS, component 2
Coefficient of determination (R^2_{jack})	0.88	0.78
Root mean squared error of prediction (RMSEP)	0.88 ºC	0.72 ºC
Maximum bias	0.79 ºC	0.79 ºC

777
778
779
780
781
782
783
784
785
786
787
788
789
790
791
792
793
794

FIGURES

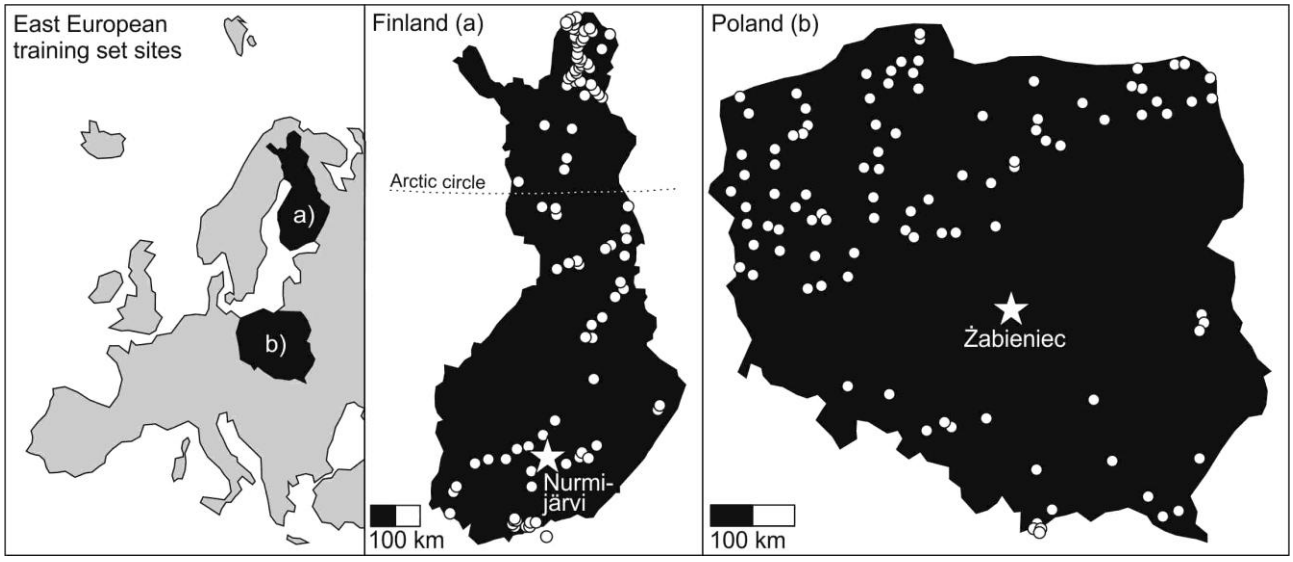

Fig. 1. Calibration sites of the East European chironomid-based temperature training set. The Finnish dataset (60°13'–69°55'N) include 114 (a) and the Polish dataset (49°19'–54°68'N) 98 lakes (b). The downcore study site Żabieniec (Poland) and Nurmijärvi (Finland) are marked with stars.

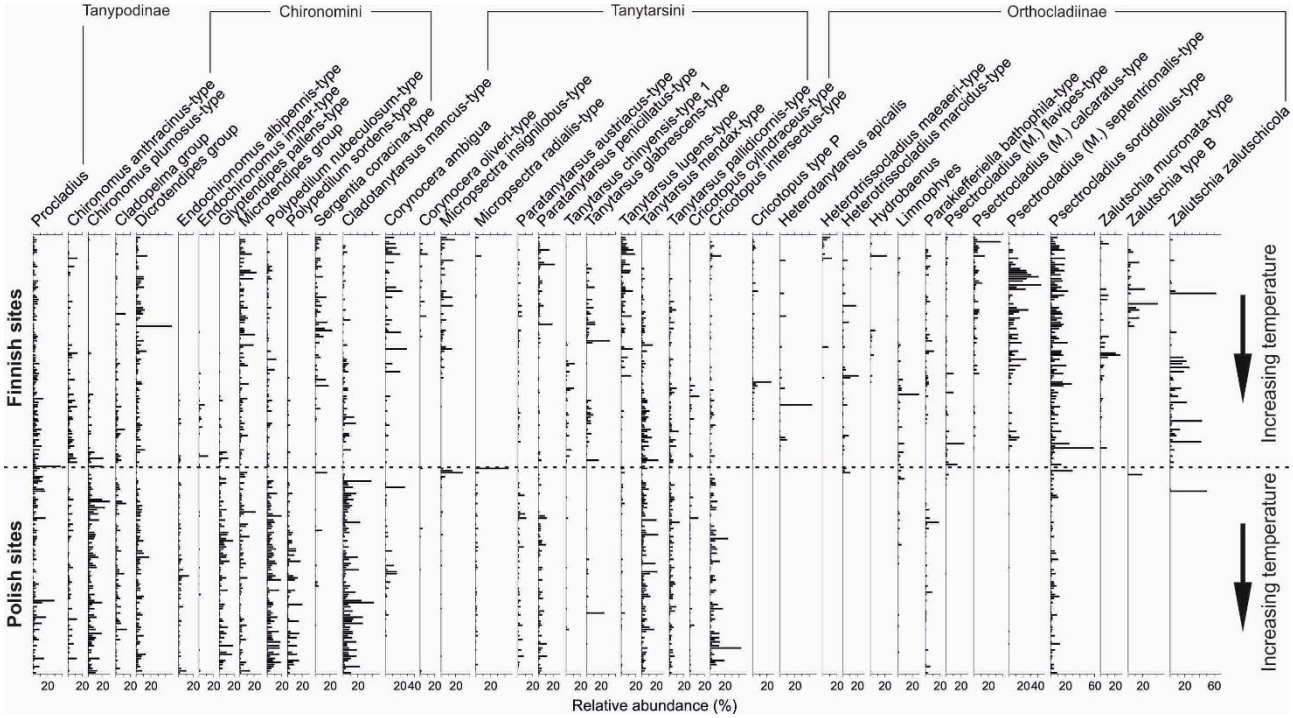

Fig. 2. Most common chironomid taxa (>10 occurrences and maximum abundance >10%) in the combined East European chironomid-temperature training set.

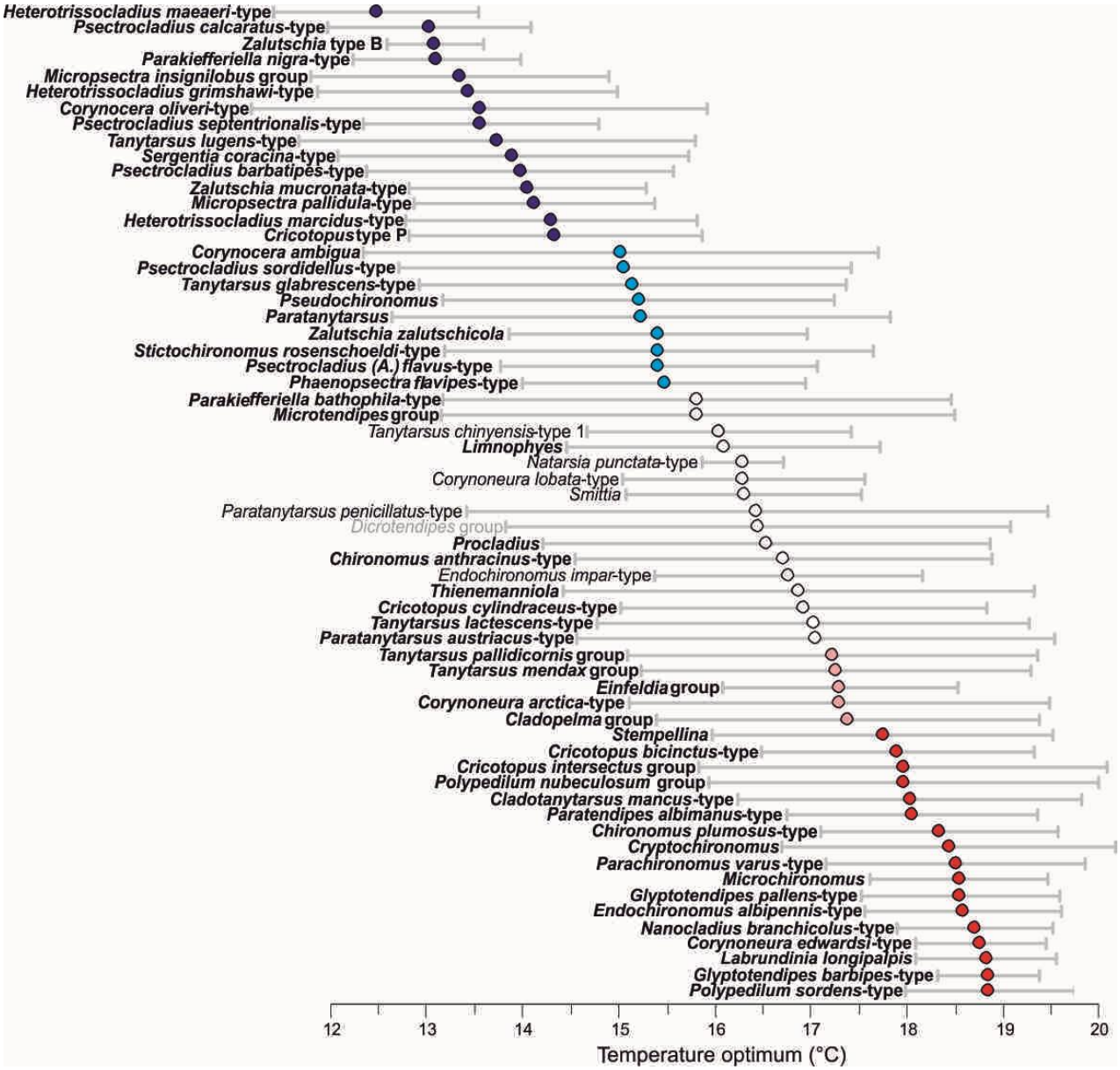

Fig. 3. Chironomid mean July air temperature optima (weighted averaging) of the most common taxa (N > 5) in the combined East European dataset. The cold indicators are marked with blue, intermediate taxa with white and warm indicators with red. Taxa having statistically significant linear relationships with temperature are marked in bold type and nonlinear fit with regular font. The only taxon (*Dicrotendipes*) with no significant relationship is marked in grey.

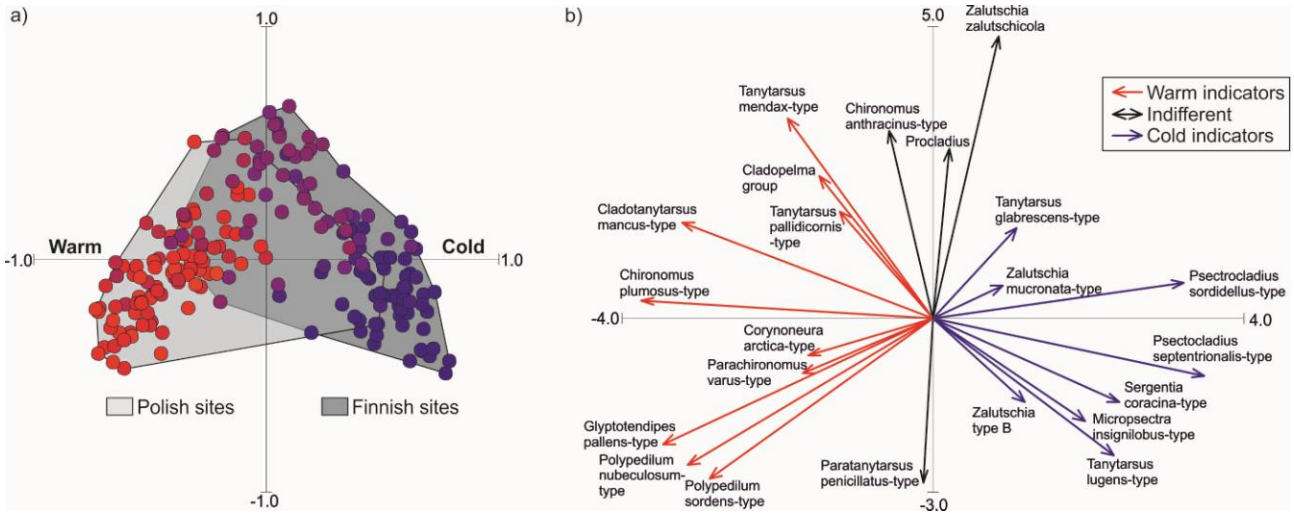

Fig. 4. Principal Component Analysis (PCA) ordination plots for samples (a) and selected taxa (b) based on surface sediment chironomid assemblages from lakes in Poland and Finland. The first (horizontal) PCA axis ($\lambda = 0.20$) explains 19.7% and the second (vertical) PCA axis ($\lambda = 0.07$) 6.6% of the total variance. The samples (sites) are colored according to their temperature from warm (red) to cold (blue) and the envelopes represent the different geographical regions.

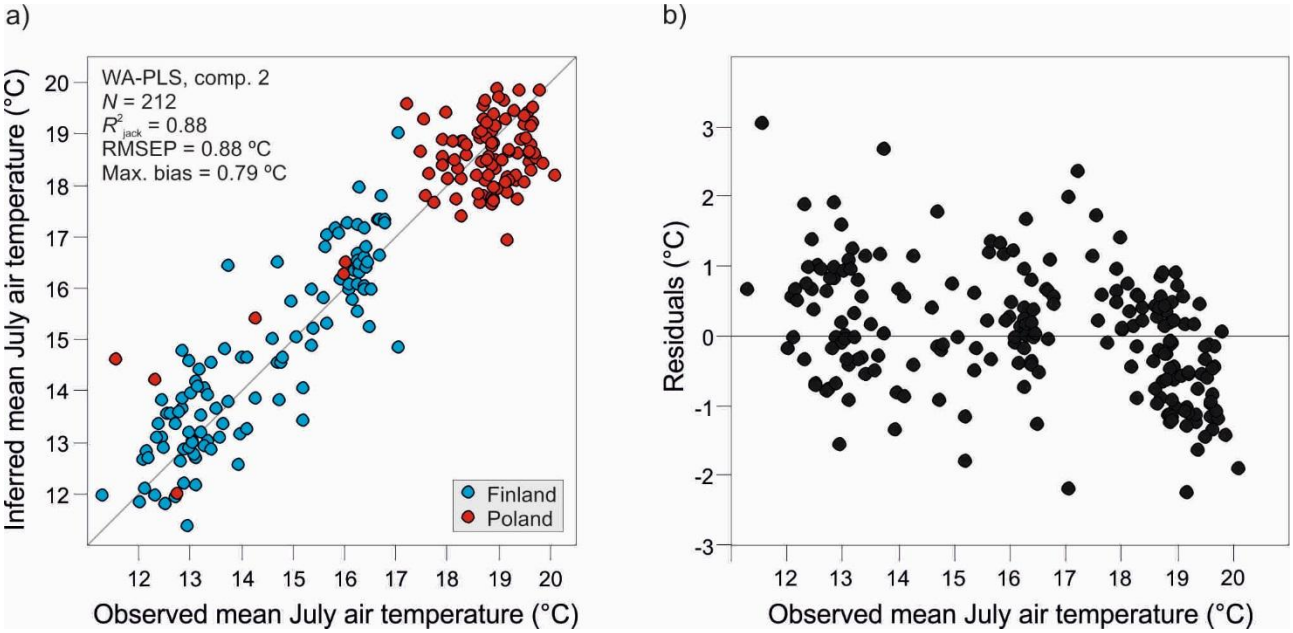

834

835 Fig. 5. (a) Relationship (1:1) between observed and chironomid-inferred mean July air temperatures
836 in the East European calibration model using the Weighted Averaging-Partial Least Squares (WA-
837 PLS) technique with two regression calibration components. N = number of calibration sites, R^2_{jack}
838 = jackknife cross-validated correlation coefficient, RMSEP = root mean squared error of prediction.
839 (b) Residuals versus observed temperatures.

840

841

842

843

844

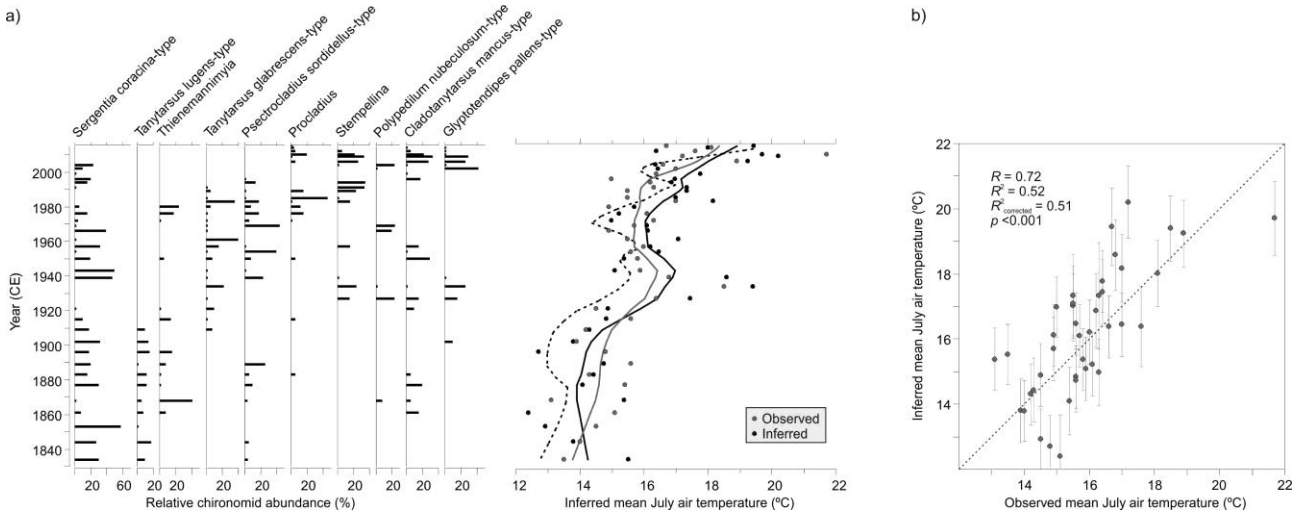

Fig. 6. Ten most common chironomids (Luoto & Ojala 2017) and chironomid-inferred mean July air temperature reconstruction from Lake Nurmijärvi (southern Finland) using the East European calibration model compared with instrumentally measured temperatures (a) and their 1:1 relationship with sample-specific error estimates using bootstrapping cross-validation (b). The dashed curve is the smoothed (LOESS span 0.2) original reconstruction using the Finnish model (Luoto & Ojala 2017). The taxa are ordered according to their temperature optima in the calibration set from the coldest to warmest.

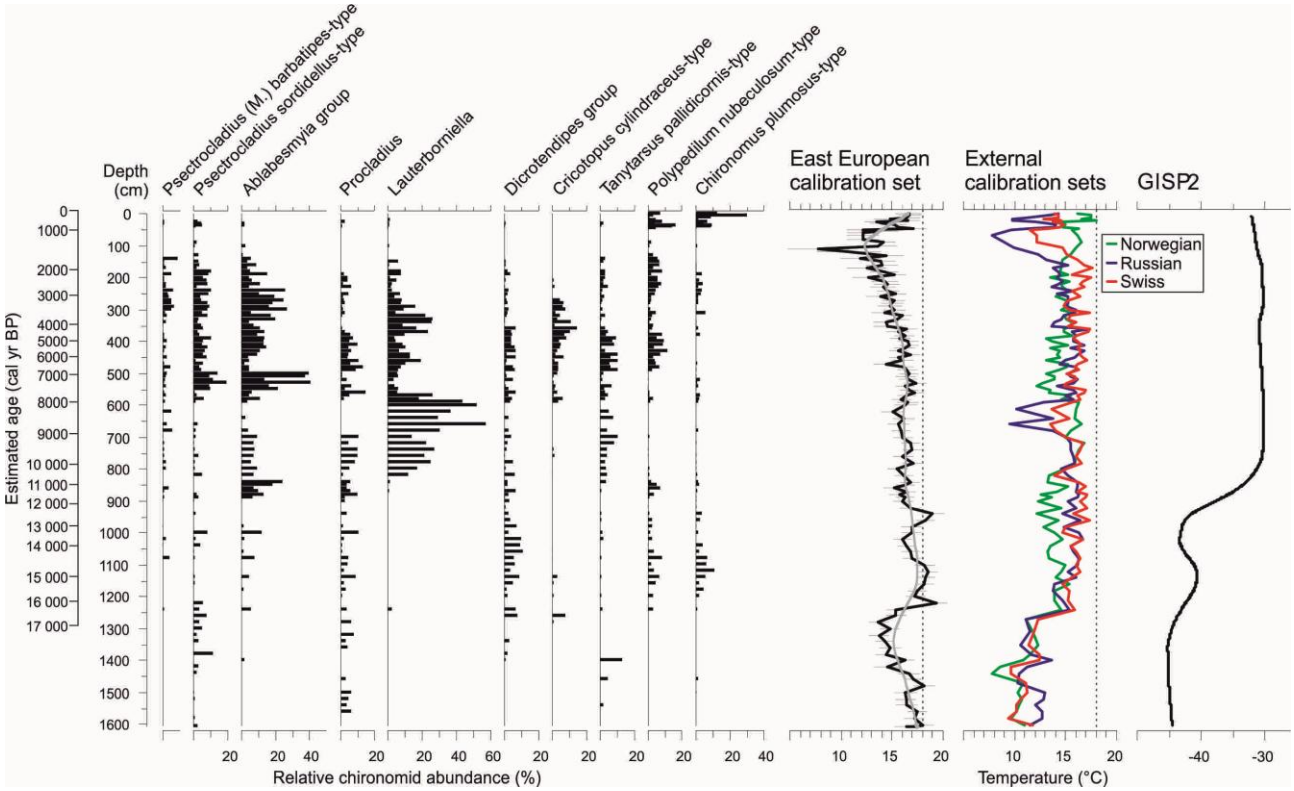

Fig. 7. Ten most common chironomids (Płóciennik et al. 2011) and chironomid-inferred mean July air temperature reconstruction from Żabieniec paleolake (Poland) using the East European calibration model compared with reconstructions (Płóciennik et al. 2011) using the Norwegian, Swiss and Russian calibration datasets. The taxa are ordered according to their temperature optima in the calibration set from the coldest to warmest. The gray line in the new reconstruction represent LOESS smoothing (span 0.2) and the error bars represent the bootstrap estimated sample-specific errors. Modern temperature at the study site is drawn as dashed lines. The smoothed (0.2) Greenland ice core data (GISP2, Cuffey & Clow 1997; Alley 2000) is provided to illustrate hemispheric temperature development (note that the timescale is only tentative due to chronological uncertainties).